PCCP

PAPER

Cite this: *Phys. Chem. Chem. Phys.*, 2017, **19**, 7101

Partitioning of caffeine in lipid bilayers reduces membrane fluidity and increases membrane thickness

Adree Khondker,†[a] Alexander Dhaliwal,†[a] Richard J. Alsop,[a] Jennifer Tang,[a] Matilda Backholm,[ab] An-Chang Shi[a] and Maikel C. Rheinstädter*[a]

Received 28th November 2016,
Accepted 10th February 2017

DOI: 10.1039/c6cp08104e

rsc.li/pccp

Caffeine is a small amphiphilic molecule, which is widely consumed as a stimulant to prevent fatigue, but is also used as a common drug adjuvant in modern medicine. Here, we show that caffeine interacts with unsaturated lipid membranes made of 1-palmitoyl-2-oleoyl-*sn*-*glycero*-3-phosphocholine (POPC). By combining X-ray diffraction and molecular dynamics simulations, we present evidence that caffeine partitions in lipid membranes and locates at the head group–tail group interface of the bilayers. By attracting water molecules from neighboring lipid molecules, it leads to the formation of "water pockets", *i.e.*, a local increase of water density at this interface. Through this mechanism, caffeine leads to an overall decrease of the gauche defect density in the membranes and an increase of membrane thickness, indicating a loss of membrane fluidity. These non-specific membrane interactions may increase the efficacy of analgesic drugs through changes in the bioavailability and rate of metabolism of these drugs.

1 Introduction

Caffeine (1,3,7-trimethylxanthine) is well known for being one of the world's most widely used and safest psychoactive drugs, promoting wakefulness and attentiveness.[1–4] Additionally, caffeine and other methylxanthine compounds are present in a large number of medications as an adjuvant[5,6] to improve their therapeutic benefit.[7,8] Caffeine is also known for acting as a diuretic, causing short-term urine output and impacting the fluid balance in the body.[9]

Caffeine is a small amphiphilic molecule. It is often used as an additive to enhance analgesics, such as aspirin, ibuprofen, and acetominophen, though the exact mechanism is still a matter of debate. Three different mechanisms are currently being discussed: (1) caffeine is speculated to have analgesic properties itself. There is evidence that caffeine has anti-nociceptive activity through the inhibition of cyclo-oxygenase-2 (COX) enzyme synthesis.[10,11] (2) Caffeine could lead to increased efficacy of analgesic drugs by inhibiting oxidation of the drug in the liver. Caffeine has been found to modulate the activity of the cytochrome P450 family of metabolic enzymes in the liver.[12–16] (3) Low to moderate caffeine doses are considered to have a positive impact on general mood and performance, by inhibiting the binding of both adenosine and benzodiazepine receptor ligands to neuronal membrane-bound receptors.[17]

In addition to its specific interactions, caffeine was also found to interact reversibly with membranes. By determining the refractive index of membranes in Langmuir–Blodgett experiments, caffeine was found to partition in lipid membranes.[18] However, little is known about the molecular interaction of caffeine with membranes. Such an interaction is important to understand its pharmacological properties and impact on drug distribution, transport, accumulation, partitioning, and metabolism.[19] From Molecular Dynamics (MD) simulations, Paloncýová *et al.* reported that caffeine partitions in lipid bilayers made of POPG and DOPC and accumulates in the membrane, with the majority localized just below the head group region, at 16 Å away from the bilayer center.[20,21]

By combining X-ray diffraction and MD simulations, we show that caffeine partitions in lipid membranes and locates in the head group–tail group interface. Caffeine has a significant effect on membrane hydration: by attracting water molecules, it leads to the formation of water pockets at its location in the hydrophilic to hydrophobic interface. However, as the corresponding hydration water molecules are drawn from neighboring lipid molecules, caffeine was found to lead to an overall dehydration and thickening of the membranes.

[a] *Department of Physics and Astronomy, McMaster University, ABB-241, 1280 Main Street West, Hamilton, Ontario L8S 4M1, Canada. E-mail: rheinstadter@mcmaster.ca; Fax: +1-(905)-546-1252; Tel: +1-(905)-525-9140-23134*

[b] *Department of Applied Physics, Aalto University, Helsinki, Finland*

† These authors contributed equally to this work.

2 Results

Highly oriented, multi-lamellar membrane stacks were prepared for the X-ray diffraction experiments and analogous systems were constructed for MD simulations, such that the results between experiments and simulations could be directly compared. Caffeine was added at a concentration of 3 mol%. In order to investigate its effect on membrane hydration in detail, bilayers were hydrated at different relative humidities (RH) of 85%, 93%, and 97% in experiments and simulations. All membranes were scanned and simulated at a temperature of $T = 28$ °C.

2.1 X-ray diffraction

Multi-lamellar membrane stacks were prepared on silicon wafers, as detailed in the Materials and methods section, and their molecular structure was studied using high resolution X-ray diffraction. By using highly oriented bilayers, the in-plane ($q_\parallel$) and out-of-plane (q_z) structural features could be observed separately.

Out-of-plane diffraction data for pure POPC and POPC + 3 mol% caffeine are shown in Fig. 1(a) for 93% RH as an example. A series of well developed Braggs peaks along q_z indicates of well organized lamellar bilayers. The lamellar spacing, d_z, *i.e.*, the average distance between two bilayers within the stack, is calculated from the distance between the peaks as $d_z = 2\pi/\Delta q_z$.

Electron density profiles, $\rho(z)$, were calculated from the Fourier decomposition of the Bragg peaks, as shown in Fig. 1(b). The central minimum represents the terminal methyl groups of the lipid acyl chains, while the maximum at $z \sim 20$ Å represents the electron-rich phosphate region within the head group of the lipids. The electron density was found to be increased at z values of $|z| \sim 17$ Å in the presence of 3 mol% caffeine. The difference curve is shown in part (c) and was used to determine the average position of caffeine in the POPC bilayers.

Out-of-plane scans were measured as function of time for relative humidities of 85, 93 and 97%. The membranes were kept at a very low humidity of 10% for two days prior to the measurements to dehydrate the membranes and provide reproducible experimental conditions between different samples for the swelling experiments. Swelling of the bilayers was then observed by measuring quick diffraction scans. Fast reflectivity curves (~13 min) were obtained for pure POPC membranes and POPC + 3 mol% caffeine over a period of ~24 h. The lamellar spacing, d_z, was calculated from the first three Bragg peaks and is plotted in Fig. 2(a). As d_z is the sum of membrane thickness and hydration water layer thickness, electron densities were calculated from each reflectivity curve, and the membrane thickness, d_{HH}, and the thickness of the water layer, d_w, were determined. The results are plotted in Fig. 2(b) and (c).

While POPC and POPC + 3 mol% caffeine membranes were found to swell at 97% and 93%, no swelling was observed when membranes were exposed to 85% RH. Caffeine was found to reduce membrane swelling significantly at 93% and 97% RH, as shown in the d_z curves in Fig. 2(a).

The mechanism of membrane swelling becomes more obvious when studying d_w and d_{HH}. At 97% RH, membrane swelling in pure POPC is almost entirely caused by an increase in the hydration water thickness, as indicated by the strong increase in d_w, while d_{HH} stays almost constant. Membrane swelling in the presence of caffeine, however, was mainly the result of an increase in membrane width, d_{HH}. While the lamellar spacing, d_z, is significantly reduced in the presence of caffeine, the membrane thickness is increased, as compared to pure POPC bilayers. These observations indicate that caffeine

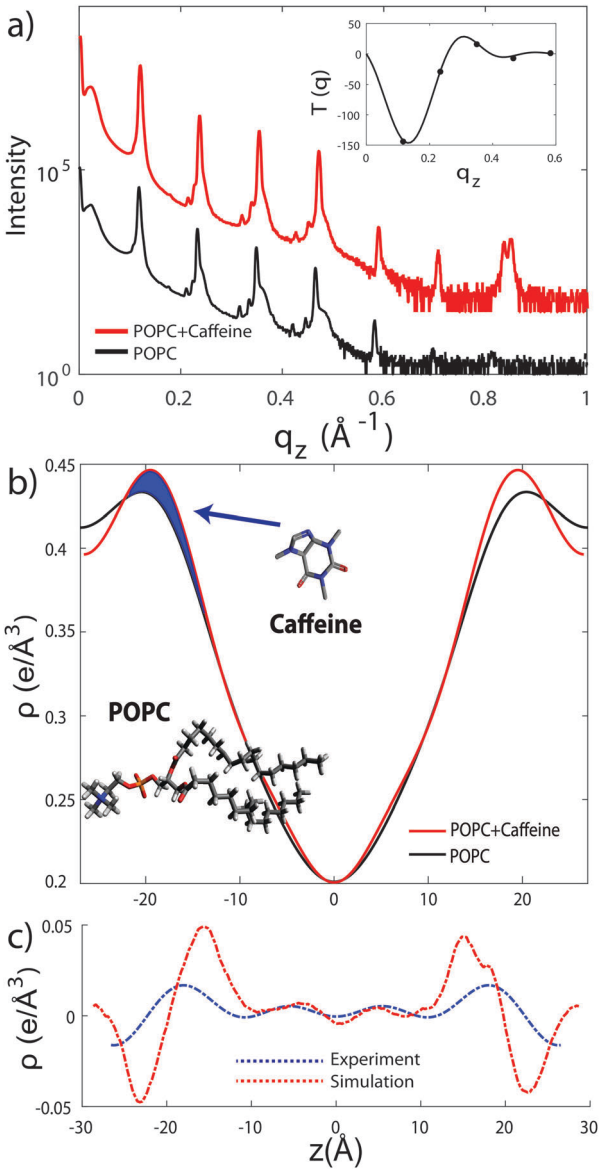

Fig. 1 (a) Out-of-plane scattering for POPC and POPC + 3 mol% caffeine, measured at 93% RH. A series of well developed Bragg peaks along q_z is observed, indicative of well organized lamellar membranes. The lamellar spacing, d_z, is determined from the distance between two Bragg peaks. The inset shows the T-function, which was used to assess the phases. (b) Electron density profiles for membranes with (red) and without (black) caffeine were generated through Fourier synthesis of the out-of-plane diffraction peaks. The increase of electron density is due to the presence of caffeine molecules in the bilayers. (c) Difference curve from (b) between POPC and POPC + 3 mol% caffeine. The peak at $|z| \sim 17$ Å marks the position of caffeine in the bilayers. The experimentally determined position is in good agreement with the position determined from MD simulations.

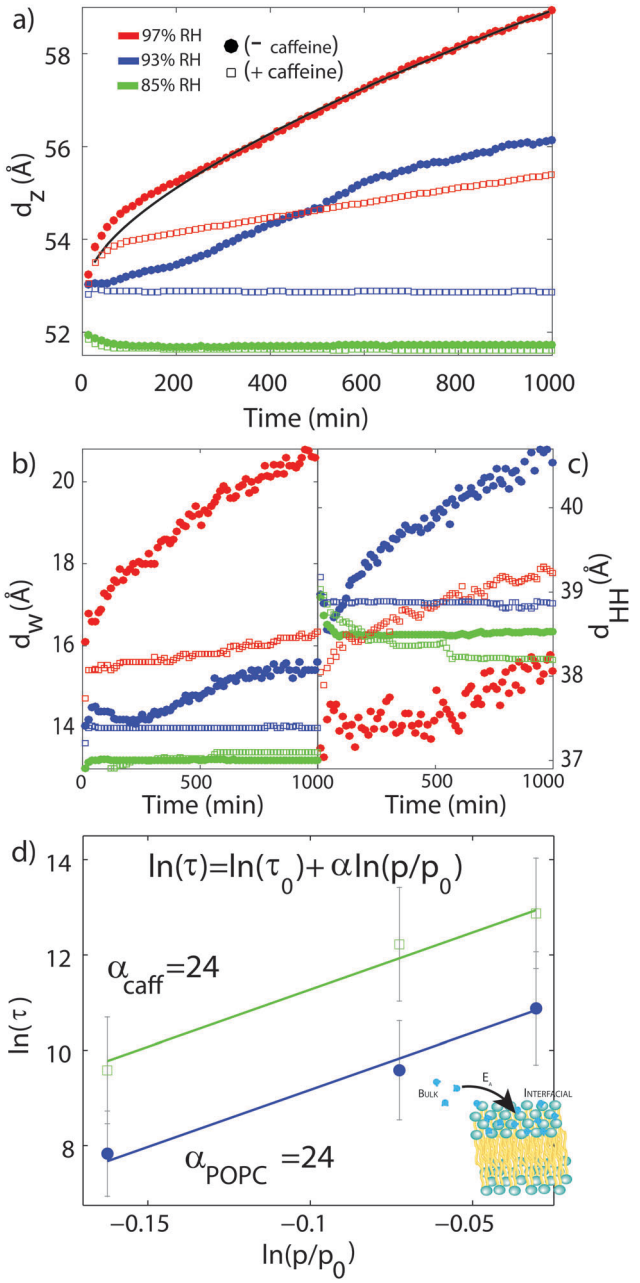

Fig. 2 Lamellar spacings as function time. (a) Time evolution of d_z for POPC (filled symbols) and POPC + 3 mol% caffeine (open symbols) for membranes hydrated in 97, 93 and 85% relative humidity. The solid line is an exponential fit ($A(1 - e^{t/\tau})$), which well described the data at times greater than 300 min. Hydration water layer thickness, d_w (b) and membrane thickness, d_{HH}, (c) as functions of time. d_w and d_{HH} were determined from the electron density profiles in Fig. 1. While POPC and POPC + 3 mol% both swell at 97% RH, the increase in d_z in pure POPC is mainly due to the increase in hydration water layer thickness, while the main mechanism for swelling in the presence of caffeine is an increase in membrane thickness. (d) Relaxation times τ (in seconds) as function of $\ln(p/p_0)$. The fit $\ln(\tau) = \ln(\tau_0) + \alpha \ln(p/p_0)$ produces a straight line indicating that the effect of the relative humidity on hydration water diffusion is independent of the presence of caffeine.

has a distinct effect on the interaction and distribution of hydration water in lipid membranes.

A relative humidity p/p_0 creates an osmotic pressure $\Pi_{osm} = (k_BT/v_w)\ln(p_0/p)$, where v_w is the partial molar volume of a water molecule.[22] In membranes, this osmotic pressure leads to an attractive potential, which is proportional to the thickness of the hydration water later, $V(d_w) = \Pi_{osm} d_w$.

The observed membrane swelling, *i.e.*, the absorption of hydration water molecules from the surrounding water vapor, is the result of water molecules migrating into the membrane stack and leading to an increase in hydration water layer thickness against the attractive forces between neighboring bilayers in the stack. As the chemical potential of water molecules is reduced by $\Delta\mu_w = k_BT\ln(p/p_0)$, this process is slowed down or completely inhibited at reduced humidity levels. It could be argued that this change in chemical potential results in an energy barrier for the water molecules to diffuse into the bilayer, $\Delta E \propto \Delta\mu_w = k_BT\ln(p/p_0)$.

The curves in Fig. 2(a) were fit to exponential functions, and the corresponding time constants, τ, were extracted and are listed in Table 1. Using Arrhenius' equation, $\tau = \tau_0 \exp(\Delta E/k_BT)$, the relaxation time depends on the energy barrier ΔE. If the extra energy barrier due to the relative humidity is given by $\Delta E = \alpha k_BT\ln(p/p_0)$, a plot of $\ln(\tau)$ would be a straight line as a function of the relative humidity $\ln(p/p_0)$, *i.e.* $\ln(\tau) = \ln(\tau_0) + \alpha\ln(p/p_0)$. As shown in Fig. 2(d), such a plot indeed produces a straight line. Furthermore, the two straight lines for POPC with and without caffeine are approximately parallel to each other, suggesting that the effect of the relative humidity on the water diffusion is independent of the presence of caffeine.

2.2 Molecular dynamics simulations

Eight systems were prepared for the MD simulations and run for 200 ns each, as listed in Table 2. The number of water molecules added to the bilayers was determined by the experiments, such that experiments and simulations could be directly compared. 12 and 11.9 water molecules per lipid molecule were used for POPC and POPC + 3 mol% caffeine systems at 85%, 12.7 and 18 for 93%, and 20 and 23.1 for 97%, respectively, in agreement with the experiments.

Snapshots of the different systems are shown in Fig. 3. Simulations for pure POPC in Fig. 3 show a uniform distribution of hydration water, whereas systems containing caffeine exhibit more deviation at the water–lipid interface. When caffeine was added to the simulations, it spontaneously partitioned into the bilayers and positioned itself at the head group–tail group interface, in excellent agreement with the X-ray results and results from prior MD simulations.[20,21] As shown in Fig. 3, the caffeine molecules attracted additional hydration water molecules, thereby increasing the water density in the hydrophilic to hydrophobic interface.

Table 1 Time constants, τ, from exponential fits to the curves in Fig. 2(a) for different relative humidities RH and chemical potentials, $\Delta\mu_w$

RH (%)	$\Delta\mu_w$ (k_BT)	τ_{POPC} (s)	$\tau_{caffeine}$ (s)
97	−0.03	53 069	39 040
93	−0.07	14 507	20 399
85	−0.16	2517	1445

Table 2 Overview of the systems prepared for the MD simulations. All simulations were run for 200 ns and the last 50 ns were used for analysis. Number of hydration water molecules at the different humidities was determined experimentally using eqn (3) and membranes were hydrated using these numbers in the MD simulations. The average area of 60.7 Å^2 for POPC under full hydration is in very good agreement with the literature value of 60.5 Å^2 using the Gromos54a7 force field[58]

# POPC molecules	Caffeine mol%	# Water molecules	Water/lipid (sim)	Area per lipid (Å^2)	RH (exp) (%)	Water/lipid (exp)
128	—	1521	11.9	61.0	85	11.9
128	—	2304	18	60.9	93	18
128	—	2960	23.1	60.0	97	23.1
128	—	3840	30	60.7	100	—
128	3	1536	12	60.8	85	12
128	3	1625	12.7	60.9	93	12.7
128	3	2560	20	61.0	97	20
128	3	3840	30	60.6	100	—

The final 50 ns of each simulation were used for the analysis and determination of structural and dynamical parameters. Electron density profiles of the various system components were generated *via* number density calculations along the *z*-coordinate, and scaled using the appropriate weighting based upon the number of electrons within each component.

The calculated electron density profile for POPC + 3 mol% caffeine is shown in Fig. 4(a). This data can be decomposed into different components, such as contributions from POPC, water molecules, and caffeine. Based on this analysis, the caffeine molecules are found in the head group–tail group interface of the POPC bilayers, at $|z|$-values of $\sim$15 Å. A direct comparison between the experimental and calculated findings is shown in Fig. 1(c). The difference between experimental and simulated caffeine position of 2–3 Å is likely the result of bilayer undulations present in the bilayer stacks that are not accurately replicated using the short timescale and small patch size of the simulations. The undulation fluctuations in membranes were previously

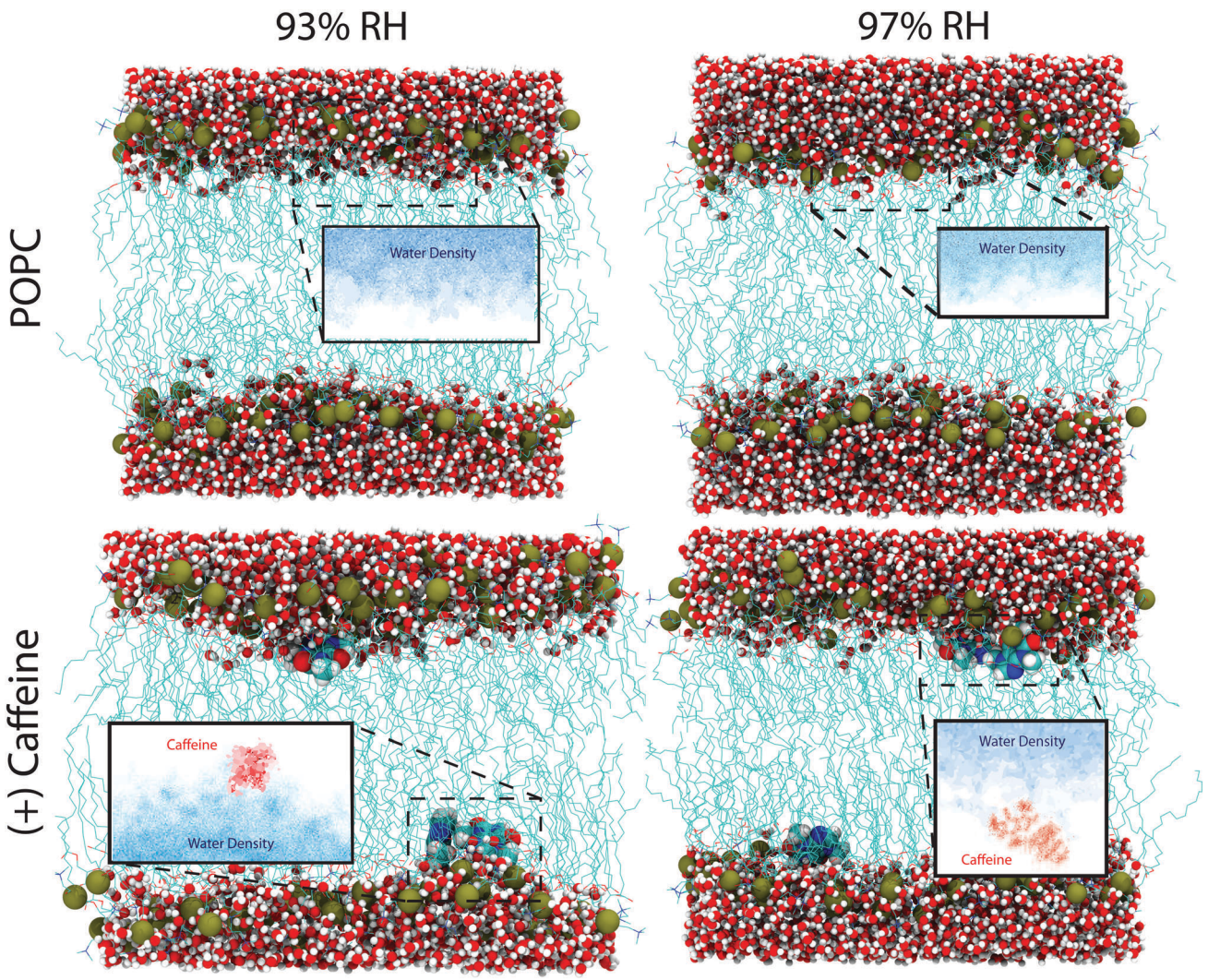

Fig. 3 MD snapshots from the simulations of POPC and POPC + 3 mol% caffeine at hydration levels of 93% and 97% RH. Simulations were run for 200 ns. The caffeine molecules were initially placed in the water layer and partitioned spontaneously into the bilayers and were found at the head group–tail group interface of the bilayers. Water density was found to be increased around the caffeine molecules.

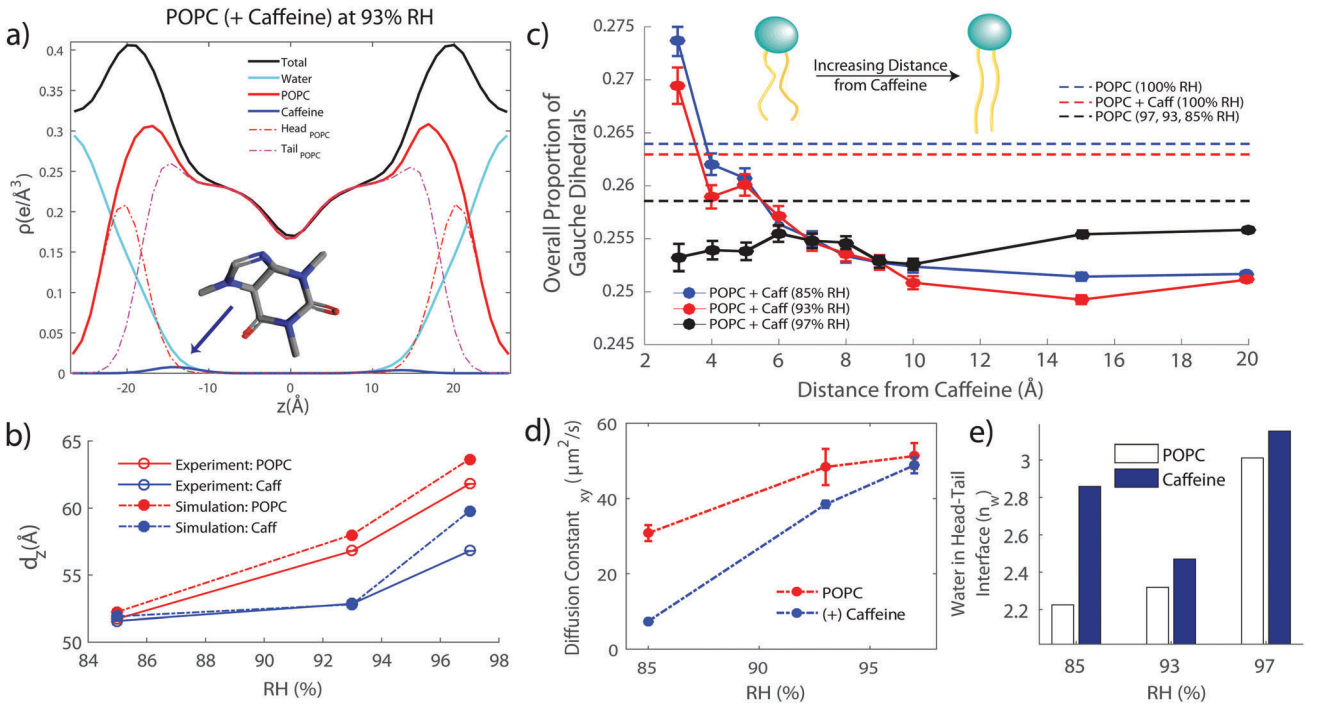

Fig. 4 Overview of the results from molecular dynamics simulations. (a) Calculated electron density profile along the bilayer normal for various electron-containing groups. Caffeine density is localized to the head group–tail group interfacial region. (b) Comparison of bilayer spacing (d_z) between experiments and simulations. Errors are in the order of 10^{-2} and smaller than symbol size. (c) Proportion of gauche dihedrals on lipid tail carbon atoms as a function of lipid distance from caffeine molecules for the three simulated hydration levels. While the number of gauche defects is significantly increased at the position of the caffeine molecules, the overall number of gauche defects is decreased, indicative of a dehydration of the membranes. Average proportions for POPC and POPC + 3 mol% caffeine at 100% RH were calculated to be 0.264 (±0.001) and 0.263 (±0.001), respectively. Pure POPC at 97, 93, and 85% RH had an average gauche proportion of 0.259 ± 0.001. (d) Average lateral diffusion constant of all lipid molecules with and without caffeine. Lateral lipid diffusion was found to be reduced for all hydration levels in the presence of caffeine. (e) Number of water molecules per lipid molecule located in the head group–tail group interface. Caffeine was found to increase water density in this region.

measured using the neutron spin-echo technique.[23,24] The corresponding undulation amplitudes can be estimated from the underlying theory of a solid supported stack of membranes by Romanov and Ulyanov[25] to about 3 Å, in good agreement with the observed deviation. A similar effect has been observed before when comparing diffraction experiment and MD simulations in the case of the interaction between cortisone and membranes.[26] The additional signals in the difference in electron density in Fig. 1(c) in the hydrophobic membrane core are likely the result of tail rearrangements in the presence of caffeine.

The width of the fully swollen bilayers for all systems is compared in Fig. 4(b). While there is a small difference in absolute d_z values, the trend as function of hydration for experimental values and simulations is in very good agreement.

To better understand the effect of caffeine on membrane fluidity, the number of gauche defects in the lipid tails, *i.e.*, kinks in the lipid alkyl chains, was calculated as a function of the lateral distance from the caffeine molecules. The results are shown in Fig. 4(c). The proportion of gauche dihedrals was analyzed using a dynamic selection of lipid molecules located within a specified radius around the caffeine molecules. The dihedral angles of the carbon within these lipid chains were analyzed and averaged across both chains. The two dihedral angles between carbons closest to the glycerol moiety did not vary significantly between systems, and thus were excluded from analysis. While the number of gauche defects was significantly increased in close proximity to the caffeine molecules, gauche defects were found to be overall reduced at larger distances in the presence of caffeine when compared to this proportion in pure POPC systems. The local increase in fluidity is more pronounced at reduced levels of hydration, where caffeine seems to have a higher affinity for the hydration water molecules.

Fig. 4(c) also depicts the average proportion of gauche defects of pure POPC for all hydration levels and POPC + 3 mol% caffeine membranes at full hydration (30 water molecules per lipid molecule) for comparison. Pure POPC at 97, 93 and 85% RH had an average proportion of 0.259 ± 0.001. Average proportions for POPC and POPC + 3 mol% caffeine at 100% hydration were calculated to 0.264 (±0.001) and 0.263 (±0.001), respectively. The proportion of gauche dihedrals is indeed highest in fully hydrated POPC bilayers and there is a significant difference between POPC at 100% RH and at 97% RH. We, therefore, argue that the gauche defect density is a good and robust measure of membrane fluidity. The comparison between POPC and POPC + 3 mol% caffeine in particular shows that caffeine reduces membrane fluidity even at full hydration of the membranes.

Lateral lipid diffusion coefficients were generated by calculating the mean squared displacement of phosphorous atoms within

the lipid head groups and fitting a linear model. Results for all hydration levels are shown in Fig. 4(d). Lipid diffusion was found to be decreased in the presence of caffeine, which is compatible with a dehydration and de-fluidification of the bilayers on a global scale.

The number of hydration water molecules in the head group–tail group interface of the bilayers was determined by integrating the water signal from the electron density profiles in Fig. 4(a) between the peaks of the head groups and the peaks of the tail groups. As the position of these peaks varied slightly from simulation to simulation, the boundaries for integration also varied, with the head and tail peaks achieving an average position of 20.34 Å and 16.71 Å for caffeine-containing bilayers, and 19.63 Å and 16.04 Å for pure POPC bilayers, respectively. The results are shown in Fig. 4(e). The data indicate that the average number of hydration water molecules in that interface is increased in the presence of caffeine at all hydration levels. The difference in additional water molecules was found to be more pronounced at lower levels of hydration.

3 Discussion

While the typical caffeine content in a 12 oz can of soda is $\sim$40 mg, a cup of coffee contains about 100 mg of caffeine. With common caffeine uptakes of $\sim$2400 mg per week, blood concentrations on the order of 3 mg L^{-1} were found,[27] corresponding to a concentration of $\sim$15 mM when using the molar mass of caffeine of 194.19 g mol^{-1}. A single 130 mg oral dose was reported to produce peak plasma concentrations of 2.5–6.8 mg L^{-1} within 20–40 min.[28] Over-the-counter supplements typically contain 100–200 mg of caffeine per tablet and doses of 32–200 mg are included in a variety of prescription drug mixtures.[29] We note that lethal doses of caffeine with blood concentrations of 200 mg L^{-1} and 600 mg L^{-1} have been reported.[29] The caffeine concentration that we used in experiment and simulations of 3 mol% corresponds to a concentration of $\sim$1 mM (when 4×10^{-7} mol of caffeine are typically added to 0.48 mL) and is, thus, absolutely comparable to typical physiological concentrations.

The interaction of caffeine with model POPC bilayers was studied using X-ray diffraction and MD simulations. Similar systems were used in both techniques, such that the results could directly be compared. 3 mol% caffeine was included in the POPC bilayers in experiment and simulations. To study the role of hydration water in the observed phenomena in detail, the membranes were studied at 85%, 93% and 97% relative humidity. The number of water molecules at the different humidities was first determined in the diffraction experiment and the same number of water molecules per lipid molecule was used in the MD simulations. Experiments and simulations were both conducted at a temperature of 28 °C.

We present experimental and computational evidence that the caffeine molecules spontaneously partition in lipid bilayers and are located in the head group–tail group interface at $|z|$-values of 17 Å in the experiment and 15 Å in the simulations. We consider this a good agreement. Small deviations between experiments and simulations have been reported before and are likely a result of undulation fluctuations, which are not accessible in the simulations due to the size of the simulation box and the accessible time scales. This membrane bound state was observed to occur spontaneously and, although some caffeine molecules entered and exited the bilayer throughout the simulation, for 99.5% of the runtime, all caffeine molecules were bound. Our findings are in excellent agreement with results from previous MD simulations,[19,30] which reported caffeine at $|z|$-positions of 16 Å.

The experimental results present evidence that POPC and POPC + 3 mol% caffeine membranes swell in different ways: the increase in lamellar spacing was smaller in the presence of caffeine on all hydration levels. While swelling in pure POPC was found to be mainly due to swelling of the hydration water layer, the thickness of the hydrophobic membrane was found to increase in the presence of caffeine. MD simulations show that the hydration water molecules are mainly located at the head group–tail group interface of the bilayers. Despite the increase of water molecules in the membranes, the bilayers were thicker in the presence of caffeine. Together with the fact that lipid diffusion is slower, these findings are compatible with a global dehydration of the bilayers.

In order to address this question in more detail, the number of gauche dihedrals was analyzed. This quantity is often used to directly indicate fluidity.[31–33] The proportion of gauche dihedrals on carbons on the tails of POPC molecules was highest in close proximity to the caffeine molecules. However, it decreased to a lower level when compared to pure POPC at further distances from the solute. This suggests that caffeine increases fluidity in its immediate vicinity, but that it has a global ordering effect with increased distance. Membranes at lower levels of hydration were more susceptible to the membrane-modulating effects of caffeine. The bilayers are less uniform in dehydrated systems, likely due to the fact that lipid rearrangement is slowed down significantly in the absence of water. We note, however, that the number of gauche defects was decreased in the presence of caffeine as compared in pure POPC, even at the highest hydration level of 97% RH.

The concept of water pockets can be used to cumulatively describe the experimental and simulated observations, as summarized in Fig. 5. The water density in the head group–tail group interface is significantly increased in membranes containing caffeine. This is the result of caffeine attracting water molecules to its location in the bilayer, creating local deviations in the bilayer surface with increased water density. As these water molecules are drawn from neighboring lipid molecules, caffeine leads to a dehydration of the neighboring membrane. As a result, the membranes containing caffeine exhibit an overall decreased fluidity and thickening across the entire bilayer when compared to membranes without caffeine.

Although caffeine is often used directly within drug regimens for its effects as a stimulant, its adjuvant properties alongside analgesic drugs like aspirin and ibuprofen are less well understood.[34,35] We observed that caffeine partitions in lipid membranes and changes membrane properties. It has two distinct effects on membranes: it thickens the bilayers and makes them less fluid, *i.e.*, it leads to a decrease in the number of gauche defects. While the analgesic and

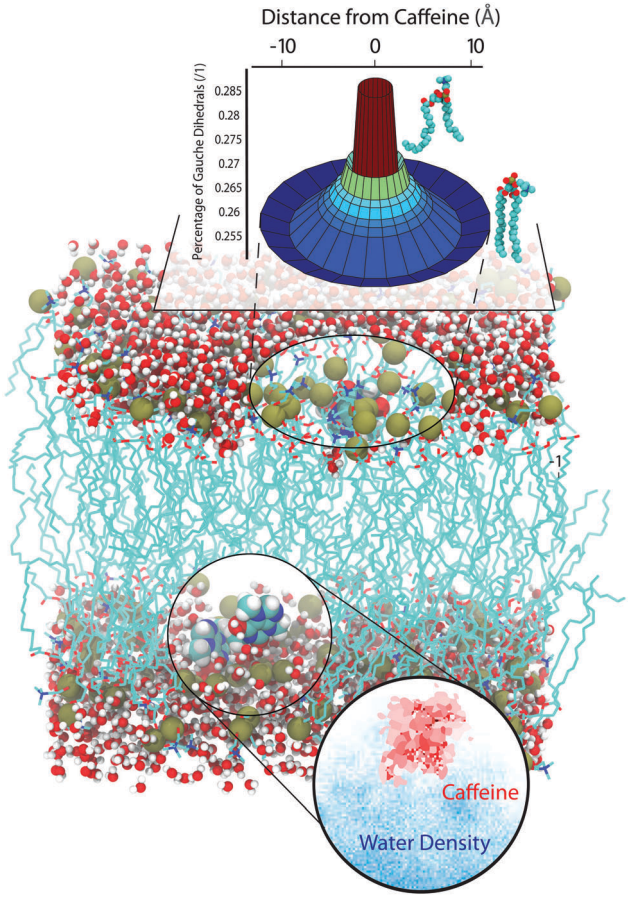

Fig. 5 Summary of the experimental and computational findings: the caffeine molecules were found to partition spontaneously in lipid bilayers and locate at the head group–tail group interface. By attracting hydration water molecules from neighboring lipid molecules, the caffeine molecules form "water pockets" in that interface. While the water density and density of lipid tail gauche defects was significantly increased in close proximity around the caffeine molecules, caffeine was found to lead to an overall dehydration and thickening of the membranes.

mood and performance increasing effect of caffeine are specific interactions, the non-specific effects of caffeine on membranes may alter the metabolism of these drugs *via* enzyme modulation.

The cytochrome P450 3A4 (CYP3A4) enzyme family is membrane-associated and inactivates exogenous and endogenous compounds, preparing them for their removal from the body. Metabolites, such as caffeine, are hypothesized to modulate the activity of cytochrome P450 enzymes in the liver.[14–16] The association of CYP3A4 with the membrane is mediated by thickening of the membrane at the contact regions close to its F/G and K/L alpha helical loops.[16] The activity of CYP3A4 depends upon the rate at which its substrates can enter its access channels, of which there are several that open into different regions of the lipid bilayer. Specific channels then select for drugs that partition to the same position across the lipid bilayer as the channel opening is located. Berka *et al.*[16] and Alsop *et al.*[36] have shown that ibuprofen partitions within the hydrophobic core of lipid bilayers, and its theorized access channel on CYP3A4 is also located within the core. The ability of caffeine to thicken membranes may raise CYP3A4's relative position when associated with the membrane, making its entrance channels less accessible to drugs, such as ibuprofen. We note that the effect of caffeine is drug dependent, as it was found to increase the depletion of acetaminophen.[12–15]

The ability of caffeine to alter the thickness of membranes may, therefore, influence the stability of metabolizing complexes and provide a potential mechanism for an interaction with analgesics by altering their bioavailability and rate of metabolism.

4 Conclusion

We studied the interaction between caffeine and unsaturated model lipid bilayers made of POPC. By combining X-ray diffraction and MD simulations, we find that caffeine molecules spontaneously partition into the head group–tail group interface of the membranes and draw additional water molecules into this interface. While pure POPC membranes typically swell through an increase in hydration water layer thickness, membranes were found to have an increased bilayer thickness and a reduced number of gauche defects in the presence of caffeine. Our findings suggest that caffeine decreases membrane fluidity globally through the formation of local water pockets at the hydrophilic to hydrophobic interface. Caffeine's effects on membrane thickness and fluidity may in particular play a role for its use as a drug adjuvant and diuretic action by affecting protein function and permeability.

5 Materials and methods

5.1 Preparation of the highly-oriented multi-lamellar membrane complexes

Highly-oriented multi lamellar membranes were prepared on single-side polished silicon wafers (1×1 cm^2). 1-Palmitoyl-2-oleoyl-*sn-glycero*-3-phosphocholine, (POPC, Avanti Polar Lipids) and caffeine (1,3,7-trimethylxanthine, Sigma) were mixed at the desired molecular ratio and dissolved in a 1 : 1 mixture of chloroform (Caledon)/2,2,2-trifluoroethanol (TFE) (Sigma). The final solution concentration was 20 mg mL^{-1}.

The wafers were placed in 1,2-dichloromethane (Caledon) within a closed Pyrex dish and cleaned by sonication for 25 minutes, which produced a hydrophobic silicon surface. The wafers were removed and rinsed three times thoroughly with alternating methanol and 18.2 MΩ cm water. The wafers were then dried with dry nitrogen gas and placed on a tilting incubator set to 40 °C. A syringe was used to deposit ~75 μL of the POPC/caffeine solution on the wafer while the tilt (speed 15, tilt angle 1°) provided circular flow and even distribution of the solution on the wafers. The membranes were allowed to dry for 15 minutes on the tilting incubator.

This procedure resulted in highly oriented, multi-lamellar membrane stacks and a uniform coverage of the silicon wafers. About 3000 highly oriented stacked membranes with a total thickness of ~10 μm are produced using this protocol. The high sample quality and high degree of order is a prerequisite to determining in-plane and out-of-plane structure of the membranes separately.

Membrane samples were handled using the following protocol: membranes were placed in vacuum for 16–20 h after application to remove all traces of solvents. Membranes were then placed in a sealed container containing an open beaker of saturated ultra pure water saturated with K_2SO_4 (97%), and incubated for 48 h at 30 °C. The samples were then transferred to a glove box and kept at 10% RH (LiCl) for 24–48 h to dehydrate the samples prior to scanning, therefore providing reproducible starting conditions for the hydration experiments. The samples were then transferred into the humidity chamber for scanning. Samples were allowed to equilibrate in the chamber for 1 hours prior to scanning.

5.2 X-Ray diffraction experiment

Out-of-plane X-ray scattering data was obtained using the Biological Large Angle Diffraction Experiment (BLADE) in the Laboratory for Membrane and Protein Dynamics at McMaster University. BLADE uses a 9 kW (45 kV, 200 mA) CuK-α Rigaku Smartlab rotating anode at a wavelength of 1.5418 Å. Both source and detector are mounted on moveable arms such that the membranes stay horizontal during measurements. Focussing, multi layer optics provide a high intensity parallel beam with monochromatic X-ray intensities up to 10^{10} counts per (s mm^2). This beam geometry provides optimal illumination of the membrane samples to maximize the scattered signal. By using highly-oriented stacks, the in-plane ($q_{||}$) and out-of-plane (q_z) structure of the membranes could be determined independently. Out-of-plane diffraction scans permit the reconstruction of electron density profiles, which were used to determine the detailed structure of the lipid bilayer perpendicular to the membrane plane.[37]

Membrane samples were placed in a humidity chamber during the X-ray experiments. Humidity was controlled by saturated salt solutions of K_2SO_4, K_2NO_4, and KCl at 28 °C to achieve relative humidities of 97%, 93%, and 85%, respectively, during the scans. For the time dependent measurements, 125 scans at 13.33 min per scan for a period of ∼24 h were measured. For the determination of electron densities, membranes then were re-aligned and long, 3 h reflectivity scans with good statistics were measured.

The accuracy in the determination of the different lamellar spacings and the number of hydration water molecules can be estimated from the time-dependent hydration curves. The increase in hydration water layer for pure POPC at 97% RH was well fitted by an exponential increase ($\mathrm{bg} + A(1 - \exp[-(t - t_0)/\tau])$) with parameters A = 31.9 Å, τ = 53 040 s, bg = −8.8 Å, and t_0 = 85 020 s. We note that the time t_0 roughly agrees with the time the bilayers were incubated before the experiment so the membranes seem to 'remember' that they have been hydrated before, similar to aging and memory experiments.[38,39] The difference in theoretical hydration water thickness after waiting and hydrating for 1 day (86 400 s) and at 97 200 s, the time after the 3 h reflectivity scan was completed, is in both cases calculated to 23.07 Å, in excellent agreement with the experimentally determined equilibrated value of 23.1 Å.

5.3 Out-of-plane structure and electron densities

The out-of-plane membrane electron density, $\rho(z)$, can be approximated by a 1-dimensional Fourier analysis:[40,41]

$$\begin{aligned}\rho(z) &= \frac{2}{d_z}\sum_{n=1}^{N} F(q_n)\nu_n \cos(q_n z) \\ &= \frac{2}{d_z}\sum_{n=1}^{N} \sqrt{I_n q_n}\nu_n \cos\left(\frac{2\pi n z}{d_z}\right).\end{aligned} \tag{1}$$

N is the highest order of the Bragg peaks observed in the experiment. The integrated peak intensities, I_n, are multiplied by q_n to generate the form factors, $F(q_n)$. The bilayer form factor, which is in general a complex quantity, is real-valued when the structure is centro-symmetric. The phase problem of crystallography, therefore, simplifies to the sign problem $F(q_z) = \pm|F(q_z)|$, and the phases, ν_n, can only take the values ±1. The phases, ν_n are needed to reconstruct the electron density profile from the scattering data following eqn (1). When the membrane form factor $F(q_z)$ is measured at several q_z values in a continuous fashion, $T(q_z)$, which is proportional to $F(q_z)$, can be fit to the data:

$$T(q_z) = \sum_n \sqrt{I_n q_n}\,\mathrm{sinc}\left(\frac{1}{2}d_z q_z - \pi n\right). \tag{2}$$

In order to determine the phases quantitatively, the form factor has to be measured at different q_z-values using the so-called swelling technique or by measuring the bilayer at different contrast conditions when using neutron diffraction. In this paper, the phases, ν_n, were assessed by fitting the experimental peak intensities and comparing them to the analytical expression for $T(q_z)$ in eqn (2). An array of phases [−1 −1 1 −1 −1] was used for all samples. An example is shown as inset in Fig. 1(a).

The calculated electron densities, $\rho(z)$, which are initially on an arbitrary scale, were transformed to an absolute scale. For membranes at 85% and 93% relative humidity, the curves were vertically shifted to fulfil the condition $\rho(0)$ = 0.22 e$^-$ Å^{-3} (the electron density of a CH_3 group) in the center of a bilayer. The curves were then scaled until the total number of electrons $\mathrm{e}^- = A_\mathrm{L}\int_0^{\mathrm{d}z/2}\rho(z)\mathrm{d}z$ across a membrane leaflet agrees with the total number of electrons of a POPC molecule with n_w water molecules and the contribution of the caffeine molecule. An area of A_L = 64.3 Å^2 was used for the membranes at 93%.[42,43]

The number of hydration water molecules, n_w, at the different hydrations was calculated using:

$$n_\mathrm{w} = \frac{A d_\mathrm{w}}{V_\mathrm{w}}, \tag{3}$$

where $d_\mathrm{w} = d_z - d_\mathrm{HH}$. d_HH is the head–head spacing, determined by the peak in the electron density profile. The number of hydration water molecules at the different relative humidities is listed in Table 2.

For membranes at 97% relative humidity, it cannot be assumed that the density at the center of the bilayer is constant. Therefore, a different scaling scheme was applied. Using a model proposed by Petrache *et al.*,[44] the profiles are placed on an absolute scale by assuming the POPC head group is

similar in dimension to a DMPC head group, and using high precision measurements of DMPC in the gel phase. Petrache *et al.* derive:

$$A_{\mathrm{POPC}} = \frac{V_{\mathrm{POPC}} - V_{\mathrm{DMPC}}}{D_{\mathrm{c,DMPC}} + 0.5\left(D_{\mathrm{HH,POPC}} - D_{\mathrm{HH,DMPC}}\right)}, \qquad (4)$$

where A_{POPC} is the area of the POPC head group. V_{POPC} is the volume of a POPC molecule, which is taken to be 1300 Å^3,[45] and $D_{\mathrm{HH,POPC}}$ the head group–head group spacing, as measured by the experiment. V_{DMPC} is the volume, taken to be 893 Å^3, D_{HH} is the head group–head group distance (21 Å), and $D_{\mathrm{c,DMPC}}$ the chain length (16 Å) of gel phase DMPC as measured by Alsop *et al.*[46] Using this estimate for A_{POPC}, the number of water molecules can be calculated using eqn (3).

The electron densities can then be placed on an absolute scale assuming an integration of the head group density, minus water, corresponds to the number of electrons in the head group:

$$n_{\mathrm{e,headgroup}} = A_{\mathrm{L}} \int_{D_{\mathrm{C}}}^{D_z/2} (\rho(z) - \rho_{\mathrm{w}}) \mathrm{d}z = 164 + n_{\mathrm{e,caff}}. \qquad (5)$$

Caffeine's position in the bilayers was determined at a humidity of 93% where the membranes were found to be stable over time. We note that the reflectivity curves in Fig. 1(a) were measured after the membranes were hydrated for 24 h such that changes of d_z over time could be considered negligible.

5.4 Molecular dynamics simulations

All simulations were run in-house on MacSim, a GPU accelerated workstation with 20 physical Intel XeonCPU cores and two GeForce GTX 1080 high power graphics cards resulting in 5120 CUDA Cores. This system produces about 180 ns of MD simulations in standard 128 lipid membrane patches in GROMACS per day (~24 h).

A system of 128 POPC lipids (64 per leaflet) was taken from Tieleman *et al.*[47] Caffeine topology was constructed using the Automated Force Field Topology Builder (ATB), computing partial charges using quantum mechanical optimization at the B3LYP/6-31G* level of theory.[48,49] The SPC water model was used for system solvation.[50] All MD simulations were performed using the GROMACS 5.1.2 software package,[51] implementing the GROMOS 54a7 force field[52] modified with Berger lipid parameters.[53] All simulations used a 2 fs time step, a periodic boundary condition applied to all directions, the particle-mesh Ewald to solve for long-range electrostatics,[54] a short-range van der Waals cutoff of 1.2 nm, and the LINCS algorithm to determine bond constraints.[55] Temperature coupling was controlled using a Nosé–Hoover thermostat at 28 °C (τ = 0.5 ps),[56] and pressure was kept at 1.0 bar using Parrinello–Rahman semi-isotropic weak coupling (τ = 1 ps).[57] An overview of all systems prepared for the MD simulations is shown in Table 2.

The area per lipid was calculated for all systems and is included in the table. The average area of 60.7 Å^2 for POPC under full hydration is in very good agreement with the literature values of 60.5 Å^2 using the Gromos54a7 force field.[58] This area is comparable but slightly smaller than the area reported from experiments by Kucerka *et al.* of 64.3 Å^2.[42] We note that there was no statistically significant difference in the calculated areas between different samples, which is likely a consequence of the force field used. We, therefore, decided to use the gauche defect density as a local and more sensitive parameter for fluidity.

A total of six distinct simulations were conducted. Systems containing pure POPC and POPC + 3 mol% caffeine were run at 85% RH, 93% RH, and 97% RH for 200 ns each, and the final 50 ns were used for analysis. For the systems containing caffeine, the solute molecules were placed within the aqueous water layer, and the simulation was run until spontaneous insertion into the bilayer was observed. This occurred for all systems within ~20 ns. To avoid the effects of a mismatch, several systems were prepared and pre-equilibrated and only systems with a symmetric distribution of caffeine molecules were selected and eventually simulated for 200 ns. The relative humidity conditions in the experiments were replicated in the MD simulations by controlling the total number of water molecules using the experimentally determined equilibrated hydration values as inputs.

All analyses were performed with the final 50 ns of the simulations using GROMACS algorithms and simple scripts.[59] The electron density profiles were calculated for different constituents of the system, similar to other studies using lipid bilayers.[36,60] The function used calculates the relative distance along the bilayer normal of each atom within the specified index group, assigns a weighting based upon the number of electrons in each atom, and delivers an electron density as averaged over the specified time range. Because a united-atom model of POPC was used, methylene carbons in the phospholipid tails were assigned a weight of 8 electrons, and the terminal methyl of each tail was given a weight of 9 electrons. The result is shown in Fig. 4(a) using the 93% RH data as example.

The proportion of gauche dihedrals within a lipid system is commonly used as a measure of bilayer fluidity.[31–33] The proportion of gauche dihedrals as a function of increasing distance from caffeine was determined using dynamic scripting and GROMACS algorithms. A script was constructed to generate an index file containing only carbon chains belonging to lipids within the specified radius from the center of mass of any caffeine molecule within the system every 50 frames. This index file specified the POPC molecules whose carbons were to be used in calculation of the Ryckaert–Bellemans dihedral angles over that time interval. This was repeated over the final 50 ns of the simulation and averaged for each carbon position. Averaging across the SN1 and SN2 tails was then performed to generate the value shown in Fig. 4(c), and the script was run successively to consider each new distance from caffeine. Testing with the script showed that windows shorter than 50 frames did not produce statistically different results, so this frame length was used to decrease computational time. Error bars for this data were generated using the standard error of the data, calculated by taking the standard deviation of the values for the dihedral fraction and dividing by the square root of the number of data points used.

As another measure of fluidity and membrane activity, the lateral movement of lipids within the bilayer systems was characterized using a diffusion constant, $D(xy)$.[32] This was calculated by evaluating the mean square displacement of the

phosphorous atoms within the lipid head groups in the plane perpendicular to the bilayer normal and averaging:

$$\lim_{t\to\infty}\left\langle \|r_i(t) - r_i(0)\|^2 \right\rangle = 4D_{xy}t, \quad (6)$$

where the Einstein relation generalized to two-dimensions was used to solve for D_{xy}.[61] Linear regression over a time interval of 20 to 180 ns was used to calculate the diffusion constant, as all curves were most linear within this range.

Acknowledgements

This research was funded by the Natural Sciences and Engineering Research Council of Canada (NSERC), the National Research Council Canada (NRC), the Canada Foundation for Innovation (CFI) and the Ontario Ministry of Economic Development and Innovation. R. J. A. is the recipient of an NSERC PGS-D scholarship, A. D. is the recipient of an NSERC USRA, M. C. R. is the recipient of an Early Researcher Award of the Province of Ontario and a University Scholar Award from McMaster University.

References

1 J. A. Nathanson, Caffeine and related methylxanthines: possible naturally occurring pesticides, *Science*, 1984, **226**, 184–187.
2 A. Nehlig, J.-L. Daval and G. Debry, Caffeine and the central nervous system: mechanisms of action, biochemical, metabolic and psychostimulant effects, *Brain Res. Rev.*, 1992, **17**, 139–170.
3 M. Orrú, X. Guitart, M. Karcz-Kubicha, M. Solinas, Z. Justinova, S. K. Barodia, J. Zanoveli, A. Cortes, C. Lluis and V. Casado, *et al.*, Psychostimulant pharmacological profile of paraxanthine, the main metabolite of caffeine in humans, *Neuropharmacology*, 2013, **67**, 476–484.
4 A. Baratloo, A. Rouhipour, M. M. Forouzanfar, S. Safari, M. Amiri and A. Negida, *et al.*, The role of caffeine in pain management: a brief literature review, *Anesth. Pain Med.*, 2016, **6**, e33193.
5 J. Sawynok and T. L. Yaksh, Caffeine as an analgesic adjuvant: a review of pharmacology and mechanisms of action, *Pharmacol. Rev.*, 1993, **45**, 43–85.
6 J. A. Carrillo and J. Benitez, Clinically significant pharmacokinetic interactions between dietary caffeine and medications, *Clin. Pharmacokinet.*, 2000, **39**, 127–153.
7 S. Diamond, T. K. Balm and F. G. Freitag, Ibuprofen plus caffeine in the treatment of tension-type headache, *Clin. Pharmacol. Ther.*, 2000, **68**, 312–319.
8 C. J. Derry, S. Derry and R. A. Moore, Caffeine as an analgesic adjuvant for acute pain in adults, *Cochrane Database of Systematic Reviews*, 2014, CD009281.
9 R. J. Maughan and J. Griffin, Caffeine ingestion and fluid balance: a review, *J. Hum. Nutr. Diet.*, 2003, **16**, 411–420.
10 B. L. Fiebich, K. Lieb, M. Hüll, B. Aicher, J. Van Ryn, M. Pairet and G. Engelhardt, Effects of caffeine and paracetamol alone or in combination with acetylsalicylic acid on prostaglandin E2 synthesis in rat microglial cells, *Neuropharmacology*, 2000, **39**, 2205–2213.
11 W.-Y. Zhang, A benefit-risk assessment of caffeine as an analgesic adjuvant, *Drug Saf.*, 2001, **24**, 1127–1142.
12 T. Nouchi, J. M. Lasker and C. S. Lieber, Activation of acetaminophen oxidation in rat liver microsomes by caffeine, *Toxicol. Lett.*, 1986, **32**, 1–8.
13 T. F. Kalhorn, C. A. Lee, J. T. Slattery and S. D. Nelson, Effect of methylxanthines on acetaminophen hepatotoxicity in various induction states, *J. Pharmacol. Exp. Ther.*, 1990, **252**, 112–116.
14 C. A. Lee, K. E. Thummel, T. F. Kalhorn, S. D. Nelson and J. T. Slattery, Inhibition and activation of acetaminophen reactive metabolite formation by caffeine. roles of cytochromes p-450ia1 and iiia2, *Drug Metab. Dispos.*, 1991, **19**, 348–353.
15 C. A. Lee, K. E. Thummel, T. F. Kalhorn, S. D. Nelson and J. T. Slattery, Activation of acetaminophen-reactive metabolite formation by methylxanthines and known cytochrome p-450 activators, *Drug Metab. Dispos.*, 1991, **19**, 966–971.
16 K. Berka, T. Hendrychová, P. Anzenbacher and M. Otyepka, Membrane position of ibuprofen agrees with suggested access path entrance to cytochrome p450 2c9 active site, *J. Phys. Chem. A*, 2011, **115**, 11248–11255.
17 C. H. S. Ruxton, The impact of caffeine on mood, cognitive function, performance and hydration: a review of benefits and risks, *Nutr. Bull.*, 2008, **33**, 15–25.
18 J. J. Ramsden, Partition coefficients of drugs in bilayer lipid membranes, *Experientia*, 1993, **49**, 688–692.
19 M. Paloncýová, K. Berka and M. Otyepka, Molecular insight into affinities of drugs and their metabolites to lipid bilayers, *J. Phys. Chem. B*, 2013, **117**, 2403–2410.
20 M. Paloncýová, K. Berka and M. Otyepka, Molecular insight into affinities of drugs and their metabolites to lipid bilayers, *J. Phys. Chem. B*, 2013, **117**, 2403–2410.
21 M. Paloncýová, R. DeVane, B. Murch, K. Berka and M. Otyepka, Amphiphilic drug-like molecules accumulate in a membrane below the head group region, *J. Phys. Chem. B*, 2014, **118**, 1030–1039.
22 V. A. Parsegian and R. P. Rand, Interaction in membrane assemblies, *Struct. Dyn. Membr.*, 1995, **1**, 643–690.
23 M. C. Rheinstädter, W. Häußler and T. Salditt, Dispersion relation of lipid membrane shape fluctuations by neutron spin-echo spectrometry, *Phys. Rev. Lett.*, 2006, **97**, 048103.
24 C. L. Armstrong, W. Häußler, T. Seydel, J. Katsaras and M. C. Rheinstädter, Nanosecond lipid dynamics in membranes containing cholesterol, *Soft Matter*, 2014, **10**, 2600–2611.
25 V. P. Romanov and S. V. Ulyanov, Dynamic and correlation properties of solid supported smectic-a films, *Phys. Rev. E: Stat., Nonlinear, Soft Matter Phys.*, 2002, **66**, 061701.
26 R. J. Alsop, A. Khondker, J. S. Hub and M. C. Rheinstädter, The lipid bilayer provides a site for cortisone crystallization at high cortisone concentrations, *Sci. Rep.*, 2016, **6**, 22425.
27 D. G. Cook, J. L. Peacock, C. Feyerabend, I. M. Carey, M. J. Jarvis, H. R. Anderson and J. M. Bland, Relation of caffeine intake and blood caffeine concentrations during pregnancy to fetal growth: prospective population based study, *BMJ*, 1996, **313**, 1358–1362.
28 S. E. O'Connell and F. J. Zurzola, Rapid quantitative liquid chromatographic determination of caffeine levels in plasma after oral dosing, *J. Pharm. Sci.*, 1984, **73**, 1009–1011.

29 S. Kerrigan and T. Lindsey, Fatal caffeine overdose: two case reports, *Forensic Sci. Int.*, 2005, **153**, 67–69.

30 T. W. Sirk, E. F. Brown, A. K. Sum and M. Friedman, Molecular dynamics study on the biophysical interactions of seven green tea catechins with lipid bilayers of cell membranes, *J. Agric. Food Chem.*, 2008, **56**, 7750–7758.

31 H. Saito and W. Shinoda, Cholesterol effect on water permeability through DPPC and PSM lipid bilayers: a molecular dynamics study, *J. Phys. Chem. B*, 2011, **115**, 15241–15250.

32 C. Hofsäß, E. Lindahl and O. Edholm, Molecular dynamics simulations of phospholipid bilayers with cholesterol, *Biophys. J.*, 2003, **84**, 2192–2206.

33 R. M. Venable, B. R. Brooks and R. W. Pastor, Molecular dynamics simulations of gel (LβI) phase lipid bilayers in constant pressure and constant surface area ensembles, *J. Chem. Phys.*, 2000, **112**, 4822–4832.

34 B. P. Schachtel, J. M. Fillingim, A. C. Lane, W. R. Thoden and R. I. Baybutt, Caffeine as an analgesic adjuvant: a double-blind study comparing aspirin with caffeine to aspirin and placebo in patients with sore throat, *Arch. Intern. Med.*, 1991, **151**, 733–737.

35 J. Sawynok and T. L. Yaksh, Caffeine as an analgesic adjuvant: a review of pharmacology and mechanisms of action, *Pharmacol. Rev.*, 1993, **45**, 43–85.

36 R. J. Alsop, C. L. Armstrong, A. Maqbool, L. Toppozini, H. Dies and M. C. Rheinstädter, Cholesterol expels ibuprofen from the hydrophobic membrane core and stabilizes lamellar phases in lipid membranes containing ibuprofen, *Soft Matter*, 2015, **11**, 4756–4767.

37 J. Tang, R. J. Alsop, M. Backholm, H. Dies, A.-C. Shi and M. C. Rheinstädter, Amyloid-β 25–35 peptides aggregate into cross-β sheets in unsaturated anionic lipid membranes at high peptide concentrations, *Soft Matter*, 2016, **12**, 3165–3176.

38 A. V. Kityk, M. C. Rheinstädter, K. Knorr and H. Rieger, Aging and memory effects in β-hydroquinone-clathrate, *Phys. Rev. B: Condens. Matter Mater. Phys.*, 2002, **65**, 144415.

39 M. C. Rheinstädter, K. Knorr and H. Rieger, Aging and scaling laws in β-hydroquinone-clathrate, *Phys. Rev. B: Condens. Matter Mater. Phys.*, 2004, **69**, 144427.

40 M. A. Barrett, S. Zheng, G. Roshankar, R. J. Alsop, R. K. Belanger, C. Huynh, N. Kučerka and M. C. Rheinstädter, Interaction of aspirin (acetylsalicylic acid) with lipid membranes, *PLoS One*, 2012, **7**, e34357.

41 A. Tomohiro, A new method for determining the phase in the X-ray diffraction structure analysis of phosphatidylcholine: alcohol, *Chem. Phys. Lipids*, 2000, **107**, 93–97.

42 N. Kučerka, M.-P. Nieh and J. Katsaras, Fluid phase lipid areas and bilayer thicknesses of commonly used phosphatidylcholines as a function of temperature, *Biochim. Biophys. Acta, Biomembr.*, 2011, **1808**, 2761–2771.

43 K. Gawrisch, H. C. Gaede, M. Mihailescu and S. H. White, Hydration of popc bilayers studied by 1h-pfg-mas-noesy and neutron diffraction, *Eur. Biophys. J.*, 2007, **36**, 281–291.

44 H. I. Petrache, S. Tristram-Nagle and J. F. Nagle, Fluid phase structure of EPC and DMPC bilayers, *Chem. Phys. Lipids*, 1998, **95**, 83–94.

45 N. Kučerka, S. Tristram-Nagle and J. F. Nagle, Structure of fully hydrated fluid phase lipid bilayers with monounsaturated chains, *J. Membr. Biol.*, 2006, **208**, 193–202.

46 R. J. Alsop, R. M. Schober and M. C. Rheinstädter, Swelling of phospholipid membranes by divalent metal ions depends on the location of the ions in the bilayers, *Soft Matter*, 2016, **12**, 6737–6748.

47 D. P. Tieleman, M. S. P. Sansom and H. J. C. Berendsen, Alamethicin helices in a bilayer and in solution: molecular dynamics simulations, *Biophys. J.*, 1999, **76**, 40–49.

48 A. K. Malde, L. Zuo, M. Breeze, M. Stroet, D. Poger, P. C. Nair, C. Oostenbrink and A. E. Mark, An automated force field topology builder (atb) and repository: version 1.0, *J. Chem. Theory Comput.*, 2011, **7**, 4026–4037.

49 K. B. Koziara, M. Stroet, A. K. Malde and A. E. Mark, Testing and validation of the automated topology builder (atb) version 2.0: prediction of hydration free enthalpies, *J. Comput.-Aided Mol. Des.*, 2014, **28**, 221–233.

50 H. J. C. Berendsen, J. P. M. Postma, W. F. van Gunsteren and J. Hermans, Interaction models for water in relation to protein hydration, *Intermolecular forces*, Springer, 1981, pp. 331–342.

51 M. J. Abraham, T. Murtola, R. Schulz, S. Páll, J. C. Smith, B. Hess and E. Lindahl, Gromacs: high performance molecular simulations through multi-level parallelism from laptops to supercomputers, *SoftwareX*, 2015, **1**, 19–25.

52 N. Schmid, A. P. Eichenberger, A. Choutko, S. Riniker, M. Winger, A. E. Mark and W. F. van Gunsteren, Definition and testing of the gromos force-field versions 54a7 and 54b7, *Eur. Biophys. J.*, 2011, **40**, 843–856.

53 O. Berger, O. Edholm and F. Jähnig, Molecular dynamics simulations of a fluid bilayer of dipalmitoylphosphatidylcholine at full hydration, constant pressure, and constant temperature, *Biophys. J.*, 1997, **72**, 2002.

54 T. Darden, D. York and L. Pedersen, Particle mesh ewald: an $N\cdot\log(N)$ method for ewald sums in large systems, *J. Chem. Phys.*, 1993, **98**, 10089–10092.

55 B. Hess, H. Bekker, H. J. C. Berendsen and J. G. E. M. Fraaije, *et al.*, Lincs: a linear constraint solver for molecular simulations, *J. Comput. Chem.*, 1997, **18**, 1463–1472.

56 D. J. Evans and B. L. Holian, The Nosé–Hoover thermostat, *J. Chem. Phys.*, 1985, **83**, 4069–4074.

57 M. Parrinello and A. Rahman, Polymorphic transitions in single crystals: a new molecular dynamics method, *J. Appl. Phys.*, 1981, **52**, 7182–7190.

58 K. Pluhackova, S. A. Kirsch, J. Han, L. Sun, Z. Jiang, T. Unruh and R. A. Bockmann, A critical comparison of biomembrane force fields: structure and dynamics of model dmpc, popc, and pope bilayers, *J. Phys. Chem. B*, 2016, **120**, 3888–3903.

59 D. Van Der Spoel, E. Lindahl, B. Hess, G. Groenhof, A. E. Mark and H. J. C. Berendsen, Gromacs: fast, flexible, and free, *J. Comput. Chem.*, 2005, **26**, 1701–1718.

60 M. B. Boggara and R. Krishnamoorti, Partitioning of non-steroidal antiinflammatory drugs in lipid membranes: a molecular dynamics simulation study, *Biophys. J.*, 2010, **98**, 586–595.

61 M. P. Allen and D. J. Tildesley, *Computer simulation of fluids*, Oxford Science Publications, 1987.